Normal peroxisome development from vesicles induced by truncated Hansenula polymorpha Pex3p

Faber, KN; Haan, GJ; Baerends, RJS; Kram, AM; Veenhuis, M

Published in:
The Journal of Biological Chemistry

DOI:
10.1074/jbc.M112347200

Publication date:
2002

THE JOURNAL OF BIOLOGICAL CHEMISTRY
Vol. 277, No. 13, Issue of March 29, pp. 11026–11033, 2002

Printed in U.S.A.

Normal Peroxisome Development from Vesicles Induced by Truncated *Hansenula polymorpha* Pex3p*

Received for publication, December 24, 2001
Published, JBC Papers in Press, January 14, 2002, DOI 10.1074/jbc.M112347200

Klaas Nico Faber‡, Gert Jan Haan§, Richard J. S. Baerends¶, Anita M. Kram‖, and Marten Veenhuis**

From Eukaryotic Microbiology, Groningen Biomolecular Sciences and Biotechnology Institute (GBB), University of Groningen, Postbus 14, 9750 AA Haren, The Netherlands

We show that the synthesis of the N-terminal 50 amino acids of Pex3p ($Pex3p_{1–50}$) in *Hansenula polymorpha pex3* cells is associated with the formation of vesicular membrane structures. Biochemical and ultrastructural findings suggest that the nuclear membrane is the donor membrane compartment of these vesicles. These structures also contain Pex14p and can develop into functional peroxisomes after subsequent reintroduction of the full-length Pex3p protein. We discuss the significance of this finding in relation to peroxisome reintroduction, *e.g.* in case peroxisomes are lost due to failure in inheritance.

Peroxisomes are remarkable among the various classes of cell organelles in that their function and abundance varies dependent on the organism, the environmental conditions, and the physiological state of the cell. Yeast are favorable model organisms to study peroxisome biogenesis because of a number of properties. Firstly, peroxisome proliferation can be strictly regulated by growth conditions, ranging from one small organelle when cells are grown in rich media containing glucose, to over 20 during growth of cells on oleate (*Saccharomyces cerevisiae*, *Yarrowia lipolytica*, and *Pichia pastoris*) or methanol (*Hansenula polymorpha*, *P. pastoris*) (1, 2). Under these conditions, peroxisomes house the key enzymes involved in the metabolism of these carbon sources. Secondly, peroxisomes are not essential for yeast cell viability when they are grown under peroxisome-repressing conditions in rich media. This feature has led to the isolation of various yeast peroxisome assembly (*pex*)-deficient mutants that are unable to utilize either oleate or methanol for growth (3–5). With few exceptions (see below), these *pex* mutant cells still contain peroxisomal membrane remnants ("ghosts"). Through genetic complementation, 23 *PEX* genes have currently been characterized (5). Data base searches using the yeast genes have presently revealed 13 human orthologues of yeast *PEX* genes. Mutations in 11 of these human *PEX* genes have been characterized and shown to be the molecular basis for inherited peroxisome biogenesis disorders, including Zellweger Syndrome, neonatal adrenoleukodystrophy, infantile Refsum's disease and rhizomelic chondrodysplasia punctata (6, 7).

The analysis of the *PEX* genes and the peroxins they encode has predominantly shed light on the molecular components involved in peroxisomal matrix protein import (reviewed in Refs. 4, 5). Relatively less is known of the biogenesis of the peroxisomal membrane and the sorting mechanisms of the proteins it contains. Earlier work showed that peroxisomal membrane proteins, like peroxisomal matrix proteins, are synthesized on free polysomes in the cytosol and are posttranslationally transported to the peroxisome (8). Together with morphological studies on peroxisome proliferation, these data have led to the hypothesis that peroxisomes develop by fission from preexisting ones (9). Recent research, however, suggested that some peroxisomal membrane proteins may travel via the ER[1] to the peroxisome and that vesicle budding and fusion processes may be involved in peroxisome growth and maturation (10–13).

Notably, the prevailing model of budding from preexisting peroxisomes cannot explain the reassembly of peroxisomes in mutant cells lacking any peroxisomal remnants (yeast and human *pex3*, *H. polymorpha per13–6^{ts}*, human *pex16*, and *Saccharomyces cerevisiae* and human *pex19*) upon functional complementation of such cells (14–21). Several recent studies have assessed the question of the origin of the peroxisomal membrane upon reappearance of the organelles in *pex*-mutants lacking peroxisomal membranes. We studied this process in a temperature-sensitive *pex* mutant of the yeast *H. polymorpha* (15). Peroxisomal membrane remnants were undetectable in these cells when grown at restrictive temperatures (43 °C). Shifting these cells to permissive conditions (37 °C) led to a rapid (within 30 min) reappearance of peroxisomes. Concurrently, South and Gould (20), Matsuzono *et al*. (19), and South *et al*. (21) studied the reappearance of peroxisomes in human cells defective for *PEX16*, *PEX19*, and *PEX3*, respectively. Peroxisomal remnants were absent in these cells also, but intact organelles were assembled upon reintroduction of the comple-

* This work was supported by a PULS Grant from the Netherlands Organization for Scientific Research through the Earth and Life Science Foundation (to K. N. F.) The costs of publication of this article were defrayed in part by the payment of page charges. This article must therefore be hereby marked "*advertisement*" in accordance with 18 U.S.C. Section 1734 solely to indicate this fact.

‡ Present address: University Hospital Groningen, Groningen University Institute for Drug Exploration (GUIDE), Division Gastroenterology and Hepatology, Hanzeplein 1, 9713 GZ Groningen, The Netherlands. E-mail: k.n.faber@med.rug.nl.

§ Supported by the Netherlands Organization for Scientific Research through the Earth and Life Science Foundation and the Netherlands Technology Foundation. Present address: Vrije Universiteit Amsterdam, Earth and Life Sciences, Molecular Microbiology, de Boelelaan 1087, 1081 HV Amsterdam, The Netherlands.

¶ Supported by the European Community. Present address: University of Groningen, Molecular Genetics, Groningen Biomolecular Sciences and Biotechnology Institute, Biological Center, Kerklaan 30, 9751 NN Haren, The Netherlands.

‖ Supported by the Netherlands Organization for Scientific Research through the Earth and Life Science Foundation and the Netherlands Technology Foundation.

** To whom correspondence should be addressed. Tel.: 31-50-363-2176; Fax: 31-50-363-8280; E-mail: M.Veenhuis@biol.rug.nl.

[1] The abbreviations used are: ER, endoplasmic reticulum; GFP, green fluorescent protein; WT, wild type; MES, 4-morpholineethanesulfonic acid; PNS, postnuclear supernatant.

TABLE I
H. polymorpha strains used in this study
Superscript ($^{1x,2x \text{ or } 3x}$) refers to the number of expression cassettes integrated in the genome of the transformed strain.

Strain	Relevant genotype	Reference
NCYC495	*H. polymorpha* WT, *leu1.1* derivative	44
RBG1	*pex3*::*URA3*, *leu1.1*	27
RBG17	*pex3*::P_{AOX}-*PEX3*^{1x}	This study
HF75	NCYC495::P_{AOX}-*PEX3*$_{[1-50]}$*GFP*^{2x}	This study
HF78	*pex3*::P_{AOX}-*PEX3*$_{[1-50]}$*GFP*^{2x}	This study
HF245	*pex3*::P_{AOX}-*PEX3*^{1x}::P_{AMO}-*PEX3*$_{[1-50]}$*GFP*^{1x}	This study
HF290	*pex3*::P_{AOX}-*PEX3*$_{[1-50]}$*β-lactamase*^{3x}::P_{AMO}-*BiP*$_{[1-30]}$*GFP*^{2x}	This study
HF305	*pex3*::P_{PEX3}-*PEX3*$_{[1-50]}$*GFP*	This study

menting gene. As suggested before by Waterham *et al.* (15), these studies revealed that peroxisomes do not necessarily derive from preexisting ones, but failed to identify the alternative origin.

Therefore, we set out to study the reappearance of peroxisomes in *H. polymorpha pex3* cells in detail upon reintroduction of full-length Pex3p, a peroxisomal membrane protein, and hybrid proteins consisting of N-terminal fragments of Pex3p and either GFP or β-lactamase. Here we show that the N-terminal 50 amino acids of Pex3p induce the formation of vesicles in the vicinity of the nuclear membrane. These Pex3p$_{1-50}$ vesicles are the specific target for peroxisome development after subsequent synthesis of full-length Pex3p.

MATERIALS AND METHODS

Strains and Growth Conditions—*H. polymorpha* NCYC495 (*leu1.1*) and derivatives of this strain (listed in Table I) were grown at 37 °C in batch cultures in YPD (1% yeast extract, 2% Bacto peptone, 2% glucose) or in mineral medium (22) containing either 0.5% (w/v) glucose, 0.5% (v/v) methanol, or a mixture of 0.1% (v/v) glycerol and 0.5% methanol as carbon and energy source in combination with 0.25% (w/v) ammonium sulfate or 0.25% (w/v) ethylamine as sole nitrogen sources. For growth on solid media, 0.67% (w/v) yeast nitrogen base was used supplemented with 1% (w/v) glucose and 2% (w/v) agar. When required, leucine was added to the media to a final concentration of 30 mg/l.

Molecular Biological Techniques—*Escherichia coli* DH5α and XL1blue were used for the propagation and amplification of plasmid DNA. Recombinant DNA procedures (enzyme digestion, cloning, plasmid isolation, PCR, and Southern blotting) were performed essentially as described by (23). Transformation of *H. polymorpha* strains and site-specific integration of single and multiple copies of plasmid DNA in the genomic *AOX*- or *AMO*-locus was performed as described (16, 24, 25).

Plasmid Constructions—Expression plasmids pHIPX4-PEX3 (26) and pHIPX4-PEX3$_{1-50}$GFP (pFEM75) (27) have been detailed before. pHIPX6-PEX3$_{1-50}$GFP (pFEM64) was obtained by inserting a 0.9-kb *Bam*HI-*Sal*I from pFEM75 into *Bam*HI-SalI-digested pHIPX6 (26), an *H. polymorpha* expression plasmid containing the *PEX3* promoter element. For co-expression of reporter genes, novel *H. polymorpha* expression vectors were constructed based on the dominant zeocin resistance gene. Vector pHIPZ4, containing the *H. polymorpha* alcohol oxidase promoter (P_{AOX}) for heterologous expression has recently been described (28). pHIPZ5, containing the *H. polymorpha* amine oxidase promoter (P_{AMO}) was constructed by inserting an 1.0-kb *Not*I-*Bam*HI DNA fragment from pHIPX5 (26) containing the P_{AMO} into *Not*I-*Bam*HI-digested pHIPZ4. pHIPZ4-PEX3$_{1-50}$β−lactamase (pFEM201) was constructed as follows. The β−lactamase reporter gene was subcloned in pBluescript II SK$^+$ (Stratagene, La Jolla, CA) as a 0.8-kb *Eco*RI-*Hin*dIII fragment from pGF154 (29) and subsequently inserted as a *Sma*I-*Sal*I fragment into pBS-*PEX3* (27) digested with *Nco*I (Klenow fill-in)-*Sal*I, resulting in pFEM32. Subsequently, a 0.15-kb PCR fragment obtained using primers per9ATG (26) and pex3-FT2 (27) was digested with *Bgl*II and *Nco*I and inserted in *Bgl*II-*Nco*I-digested pFEM32, resulting in pFEM30. The PEX3$_{1-50}$β−lactamase hybrid gene was excised from pFEM30 by *Bam*HI-*Sal*I digestion and inserted into *Bam*HI-*Sal*I-digested pHIPZ4, resulting in pFEM201. pHIPZ5-PEX3$_{1-50}$ GFP (pFEM167) was constructed by inserting a 0.9-kb *Bam*HI-*Sma*I DNA fragment from pFEM 75 (27) into *Bam*HI-*Sma*I-digested pHIPZ5. pHIPX5-*BiP*$_{1-30}$*GFP* (pFEM76) was constructed as follows. Using PCR and primers KN18 (5′-CCCAAGCTT*GGATCC* ATG TTA ACT TTC AAT AAG TC-3′) and KN19 (5′-GGGAAGCTT*AGATCT* AAA CTG CTG TGT TGT TAG TGG G-3′) a *Bam*HI site was introduced upstream the startcodon, and a *Bgl*II site downstream codon 30 (Phe) of the *H. polymorpha KAR2* gene. In addition, using PCR and primers KN14 (5′-CCCCTC GAG AAC CTG TAC TTC CAG TCG *AGA TCT* GTG AGC AAG GGC GAG GAG C-3′) and eGFP-*Sal*I (27) a *Bgl*II site was introduced upstream codon 2 (Val), and a *Sal*I site downstream the stop codon of the eGFP gene (CLONTECH). The *Bgl*II sites were used to fuse the BiP$_{1-30}$ and the eGFP genes. The flanking *Bam*HI and the *Sal*I sites were used to clone the hybrid gene downstream the amine oxidase promoter in expression vector pHIPX5.

Biochemical Methods—Crude extracts of *H. polymorpha* were prepared according to Ref. 27. SDS-PAGE (30) and Western blot analysis (31) were performed as described; blots were decorated using specific antibodies against various *H. polymorpha* proteins. The antibodies against *S. cerevisiae* Sec63p, which cross-react with the *H. polymorpha* Sec63p orthologue, were a gift from Dr. R. Schekman, Berkeley, CA. The antibodies against GFP, and *S. cerevisiae* cytosolic ADH, which cross-react with the *H. polymorpha* ADH orthologue, were a gift from Dr. W.-H. Kunau, Bochum, Germany. Goat anti-rabbit alkaline phosphatase and goat anti-rabbit horseradish peroxidase (Roche Molecular Biochemical, Almere, The Netherlands) were used as secondary antibodies, which were detected by bromo-chloroindolyl phosphate/nitro blue tetrazolium (Roche Molecular Biochemical) or ECL (Amersham Biosciences, Inc.) according to manufacturers' protocols. Enzyme activity of cytochrome *c* oxidase was determined as described (32). Protein concentrations were determined using the Bio-Rad Protein Assay system (Bio-Rad GmbH, Munich, Germany) using bovine serum albumin as standard. Cell fractionation experiments were performed as detailed by van der Klei *et al.* (33). In addition to the standard sucrose density gradients routinely used to purify peroxisomes from WT *H. polymorpha*, we used a modified gradient consisting of 4 ml 65%, 4 ml 50%, 4 ml 46%, 8 ml 40% 4 ml 35% and 4 ml 30% (w/v)-sucrose in buffer B (5 mM MES, 0.1 mM EDTA, 1 mM KCl, pH 5.5) loaded with an organellar pellet resuspended in 5 ml of homogenization buffer (5 mM MES, 0.1 mM EDTA, 1 mM KCl, 1.2 M sorbitol, pH 5.5) and centrifuged for 3 h at 33,000 × *g*.

Microscopy—Fluorescent microscopy to localize hybrid proteins containing GFP was carried out according to (27) using an Axioskop H fluorescence microscope (Zeiss Netherlands, The Netherlands) equipped with a Princeton Instruments CCD camera (RTE/CCD-1300 Y; Princeton Instruments, The Netherlands).

Whole cells and organellar fractions were fixed and prepared for electron microscopy and immunocytochemistry as described previously (34, 35). Immunolabeling was performed on ultrathin sections of unicryl-embedded cells, using specific antibodies against various *H. polymorpha* proteins, GFP and β-lactamase, and gold-conjugated goat anti-rabbit (GAR-gold) antibodies according to the instructions of the manufacturer (Amersham Biosciences, Inc.). Double immunocytochemical labeling using two polyclonal antisera and different-sized gold particles (5-nm and 15-nm GAR-gold) was performed according to Bendayan (36).

RESULTS

Synthesis of Pex3p$_{1-50}$ Causes Vesicle Formation in pex3 Cells—Similar to *pex3* cells from other organisms, *H. polymorpha pex3* cells grown in batch cultures on methanol do not contain detectable peroxisomal membrane remnants, and proteins normally residing in the peroxisomal matrix accumulate in the cytosol. However, normal peroxisomes rapidly reappear in such cells upon reintroduction of the complementing *PEX3* gene (16). In an attempt to shed light on the origin of these organelles, we introduced hybrid genes encoding N-terminal

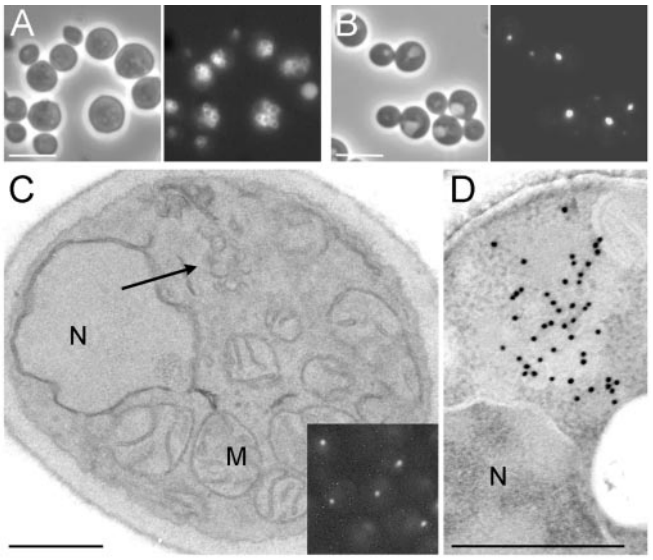

FIG. 1. **Synthesis of Pex3p$_{1–50}$GFP causes vesicle formation in pex3 cells.** Cells were grown in glycerol/methanol medium for 16 h. *A* and *B*, fluorescence microscopic analysis of HF75 (WT::P$_{AOX}$-*PEX3*$_{1–50}$*GFP*) cells (*A*) and HF78 (*pex3*::P$_{AOX}$-*PEX3*$_{1–50}$*GFP*) cells (*B*). *Left panels*, bright field images; *right panels*, fluorescent images. *C* and *D*, electron microscopic analysis of glycerol/methanol-grown HF78 cells. Membrane/vesicle clusters are observed in these cells (*C*, *arrow*), which were not found in WT control cells (not shown). The *inset* shows a fluorescent image of HF305 cells synthesizing Pex3$_{1–50}$-GFP by the *PEX3*-promoter grown in methanol-containing media. The Pex3p$_{1–50}$GFP hybrid protein is present in these membrane clusters as shown by immunolabeling using GFP-specific antibodies (*D*). *M*, mitochondrion; *N*, nucleus. *Bar* = 5 μm (*A* and *B*) and 0.5 μm (*C* and *D*).

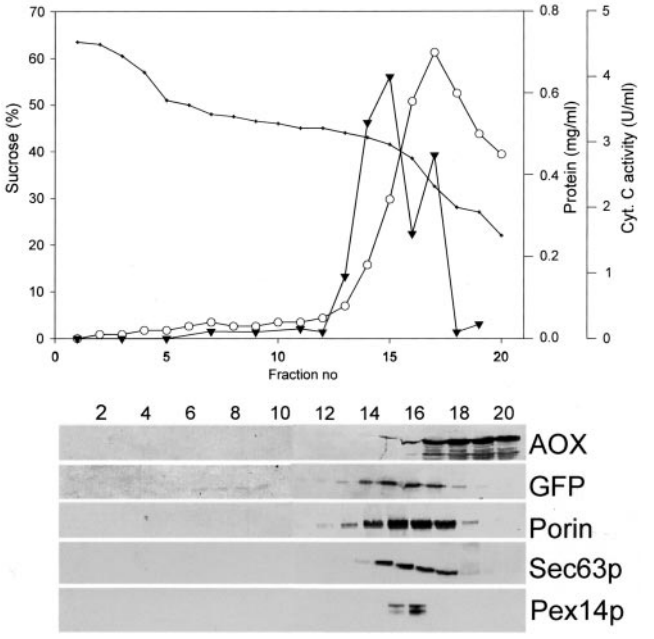

FIG. 2. **Pex3$_{1–50}$ vesicles migrate to low-density fractions after sucrose density gradient centrifugation.** Sucrose density centrifugation of a PNS obtained from glycerol/methanol-grown HF78 cells. Individual fractions were analyzed for sucrose density (+), protein concentration (○), and mitochondrial cytochrome *c* oxidase activity (▼). Western blot analysis was used to determine the location of alcohol oxidase (*AOX*), Pex3p$_{1–50}$GFP (*GFP*), mitochondrial porin, endoplasmic reticulum Sec63p, and peroxin Pex14p. All membrane-bound marker proteins co-localize in the top fractions of the gradient.

fragments of Pex3p (containing its putative peroxisomal targeting signal) and a reporter gene (GFP or β-lactamase) in *pex3* cells and determined the subcellular location of the gene products. *Pex3* cells producing the Pex3p$_{1–50}$GFP hybrid protein (strain HF78) contained one or few bright fluorescent spots (Fig. 1*B*, *right panel*); in WT controls (strain HF75) this protein was efficiently targeted to peroxisomes (Fig. 1*A*, *right panel*; Ref. 27). Electron microscopy showed that HF78 cells contained a cluster of small vesicular structures in close proximity to the nucleus (Fig. 1*C*). These structures were never observed in the *pex3* parental strain (not shown, *cf.* Ref. 16) or in WT cells. These membrane structures were the subcellular site of the Pex3p$_{1–50}$GFP hybrid protein as was shown by immunocytochemistry using α-GFP antibodies (Fig. 1*D*). The presence of these membranes was not the result of the overproduction of the hybrid protein. Similar patterns of fluorescence (Fig. 1*C*, *inset*) and membrane vesicles (not shown) were observed when the Pex3p$_{1–50}$GFP protein was produced by the *PEX3*-promoter element, though less abundantly. These data show that synthesis of the 50 N-terminal amino acids of Pex3p fused to a reporter protein, induces proliferation of membranous structures. From here, we refer to these membrane structures as Pex3p$_{1–50}$ vesicles.

Pex3p$_{1–50}$ Vesicles Display Peroxisomal Characteristics—To determine the nature of the Pex3p$_{1–50}$ vesicles, we set out to purify them, using GFP as a marker protein. The conventional biochemical procedure for the isolation of intact peroxisomes from *H. polymorpha* WT cells (homogenization of protoplasts followed by sucrose-density gradient centrifugation of a post-nuclear supernatant (PNS)) applied on HF78 cells resulted in a distinct localization of Pex3p$_{1–50}$GFP at densities of ~30–40% sucrose, colocalizing with ER and mitochondrial marker proteins (Fig. 2). To separate the Pex3p$_{1–50}$ vesicles from other cell constituents, we adjusted the sucrose density profile of the gradient to obtain a better separation at sucrose concentrations of 30–40% and loaded the gradient with an organellar fraction instead of a PNS. Fig. 3 shows that a clear separation was achieved between the Pex3p$_{1–50}$ vesicles (peak fractions at 32–36% sucrose) and the mitochondria (peak fractions at 36–42% sucrose). Comparison of the fractions most enriched for Pex3p$_{1–50}$GFP, mitochondria, and ER marker proteins (peak fractions at 38–41% sucrose) revealed that Pex14p, a peroxisomal membrane protein that is mislocalized to mitochondria in *pex3* cells (27), now co-localized with Pex3p$_{1–50}$GFP (Fig. 3*B*). This finding was further substantiated by immunocytochemical analysis of the organellar fraction (Fig. 4, *A* and *B*) and whole cells (Fig. 6*E*, see below). The Pex3p$_{1–50}$ vesicles were readily identifiable in the organellar fraction by immunocytochemistry, using specific antibodies against GFP, and were clearly distinct from other structures in these fractions, such as mitochondria and plasma membrane vesicles (Fig. 4*A*). Clearly, αPex14p-dependent-specific labeling was only found on the Pex3p$_{1–50}$ vesicles (Fig. 4*B*). In addition, co-localization of Pex3$_{1–50}\beta$-lactamase and endogenous Pex14p on the Pex3p$_{1–50}$ vesicles was observed in double-labeling experiments performed on ultrathin sections of *pex3* cells producing Pex3$_{1–50}\beta$-lactamase (Fig. 6*E*).

To further analyze the possible peroxisomal nature of the Pex3p$_{1–50}$ vesicles, we investigated whether these structures were susceptible to selective degradation, comparable with WT peroxisomes (37) and peroxisomal remnants (ghosts) in methanol-induced *H. polymorpha pex* cells (38). To this end, HF75 (WT::P$_{AOX}$-*PEX3*$_{1–50}$*GFP*) and HF78 cells (*pex3*::P$_{AOX}$-*PEX3*$_{1–50}$*GFP*) were grown in glycerol/methanol-containing media to induce peroxisome and Pex3p$_{1–50}$ vesicle formation, respectively. Next, these cells were transferred to fresh glucose media, thus repressing peroxisome and vesicle formation, and the fate of AO and GFP was followed in time. As expected, in HF75 control cells both the level of peroxisomal AO and Pex3p$_{1–50}$GFP decreased significantly (Fig. 3*C*), and after

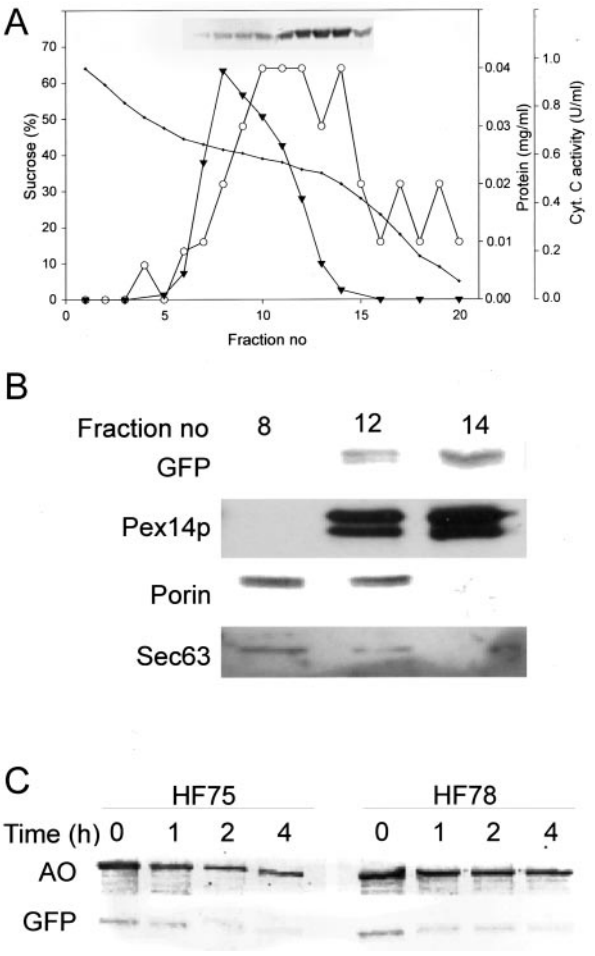

FIG. 3. **Pex3p$_{1–50}$ vesicles harbor peroxisomal characteristics.** *A*, a sucrose density gradient with an adapted sucrose density profile was used to fractionate an organellar pellet fraction prepared from glycerol/methanol-grown HF78 cells. Individual fractions were analyzed for sucrose density (+), protein concentration (○), and mitochondrial cytochrome *c* oxidase activity (▼). Western blot analysis was used to determine the location of Pex3p$_{1–50}$GFP (*top panel*). Peak fractions of mitochondria were found in fraction 8, whereas Pex3p$_{1–50}$GFP was most abundant in fraction 14. *B*, Western blot analysis of fractions 8, 12, and 14 for Pex3p$_{1–50}$GFP, Pex14p, porin, and Sec63p. Pex14p cofractionates with the Pex3p$_{1–50}$GFP vesicles. *C*, selective degradation of Pex3$_{1–50}$ vesicles; strains HF75 (WT::P$_{AOX}$-*PEX3*$_{1–50}$*GFP*) and HF78 (*pex3*::P$_{AOX}$-*PEX3*$_{1–50}$*GFP*) were grown in glycerol/methanol medium to the late logarithmic phase of growth and shifted to glucose medium, and at selected time points samples were taken. Whole cell extracts, representing equal culture volumes, were analyzed for the levels of AO and Pex3$_{1–50}$GFP by Western blotting.

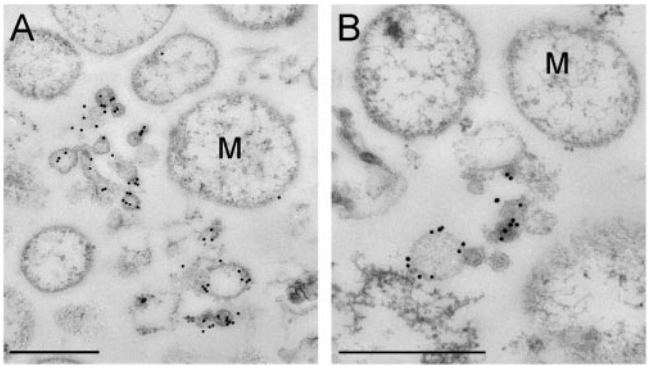

FIG. 4. **Pex14p is present on Pex3$_{1–50}$ vesicles.** Immunolabeling of the organellar fraction loaded onto the sucrose gradient analyzed in Fig. 3*A* using antibodies against GFP (*A*) and Pex14p (*B*) is shown. Typical clusters of small vesicles were specifically labeled using these antibodies. *M*, mitochondrion. *Bar* = 0.2 μm.

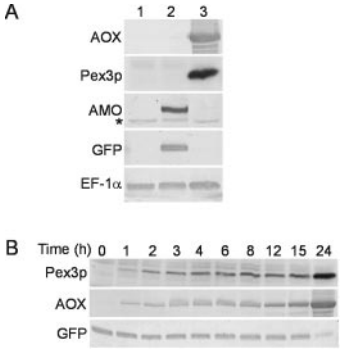

FIG. 5. **Control of protein synthesis in HF245 cells.** *A*, equal amounts of total protein extracts of HF245 (*pex3*::P$_{AOX}$-*PEX3*::P$_{AMO}$-*PEX3*$_{1–50}$*GFP*) cells grown in media containing glucose/ammonium sulfate (*lane 1*), glucose/ethylamine (*lane 2*), or methanol/ammonium sulfate (*lane 3*) were analyzed by Western blotting for the presence of AOX, Pex3p, AMO, Pex3p$_{1–50}$GFP, and elongation factor 1α (*EF-1α*; constitutively synthesized protein was used as control). Synthesis of AOX and Pex3p was specifically induced in methanol-containing media, whereas AMO and Pex3p$_{1–50}$GFP were detected only in amine-containing media. *B*, Western blot analysis of total protein extracts of HF245 (*pex3*::P$_{AOX}$-*PEX3*::P$_{AMO}$-*PEX3*$_{1–50}$*GFP*) cells shifted (at $t = 0$) from glucose/ethylamine to glycerol/methanol/ammonium sulfate medium. One hour after the shift, Pex3p and AOX are detectable, whereas Pex3p$_{1–50}$GFP (*GFP*) remains detectable even after 24 h after the shift.

4 h of induction in glucose medium, a few small peroxisomes were observed by fluorescence microscopy and electron microscopy (data not shown). In HF78 cells, however, significant amounts of AO remained detectable at this stage, showing that this cytosolic protein was not actively degraded under these conditions (39). In contrast, the level of Pex3p$_{1–50}$GFP decreased with similar kinetics as observed for HF75 cells, suggesting that the Pex3p$_{1–50}$GFP vesicles were actively degraded after a shift of HF78 cells to glucose medium. Taken together, these data suggest that the Pex3p$_{1–50}$ vesicles are not merely a sink for non-functional proteins, but instead represent membrane vesicles that show peroxisomal properties.

Pex3p$_{1–50}$ Vesicles Develop at the Nuclear Membrane—Next, we investigated the origin of the vesicles induced upon production of Pex3p$_{1–50}$GFP. To this end, we constructed a strain, HF245, in which Pex3p$_{1–50}$ vesicle production and full-length Pex3p synthesis can be separately regulated. This strain is deleted for the endogenous *PEX3* gene. Instead, it contains the *PEX3* gene under control of the methanol-inducible alcohol oxidase promoter (P$_{AOX}$) together with the gene encoding Pex3p$_{1–50}$GFP under control of the amine-inducible amine oxidase promoter (P$_{AMO}$) (Fig. 5*A*). HF245 cells were shifted from P$_{AMO}$-repressing conditions (glucose/ammonium sulfate) to media that induce the P$_{AMO}$ (glucose/ethylamine). Within 1 h after the shift, small fluorescent profiles could be detected in the cells by fluorescence microscopy. After prolonged incubation the brightness of these spots increased and only rarely we observed more than one fluorescent spot per cell (not shown, *cf.* Fig. 1*B*). Other fluorescent subcellular structures were not detected by fluorescence microscopy. A detailed electron microscopic analysis of the initial stages of the vesicle proliferation showed that these structures invariably developed in close vicinity of the nuclear membrane (Fig. 6*A*). Immunocytochemically, Pex3p$_{1–50}$GFP was solely detectable at these membranes (Fig. 6*B*). We never observed the development of a cluster of Pex3p$_{1–50}$GFP-containing membranes at another subcellular location. Similar results were obtained when GFP was replaced by β-lactamase as reporter protein. To get further insight in the donor membrane compartment of the Pex3p$_{1–50}$ vesicles, we determined whether ER-resident proteins could be detected in, or associated with, the Pex3p$_{1–50}$ vesicles by immunocytochemistry. Initial studies were performed using antisera raised

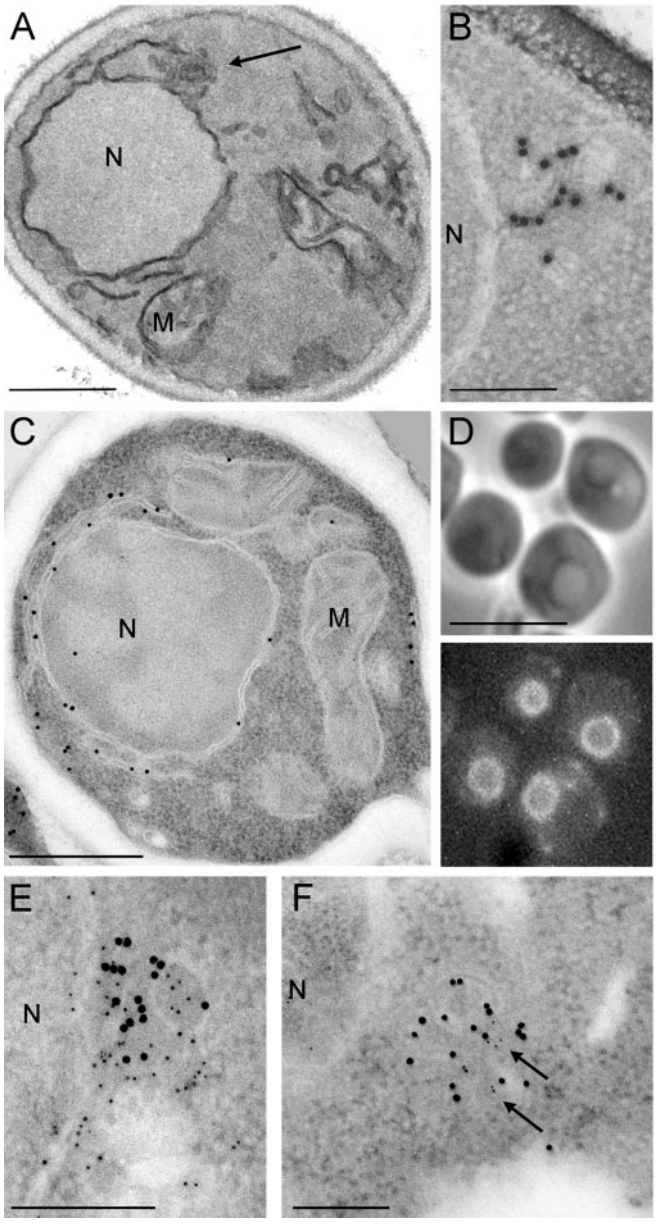

FIG. 6. **Pex3p$_{1–50}$ vesicles arise at the nuclear membrane.** *A* and *B*, electron microscopical analysis of HF245 (*pex3*::P$_{AOX}$-*PEX3*::P$_{AMO}$-*PEX3*$_{1–50}$ *GFP*) cells 1 h after a shift from glucose/ammonium sulfate to glucose/ethylamine medium. *A*, morphology. *B*, immunolocalization of Pex3p$_{1–50}$GFP using antibodies against GFP. *C–F*, ER-localized BiP$_{1–50}$GFP co-localizes with Pex3$_{1–50}$ vesicles. *C* and *D*, HF290 (*pex3*::P$_{AMO}$-*BiP*$_{1–30}$ *GFP*::P$_{AOX}$-*PEX3*$_{1–50}$β−*lactamase*) cells were grown in glucose/ethylamine medium and analyzed for the location of BiP$_{1–30}$GFP by immunocytochemistry using α-GFP antibodies (*C*) and fluorescence microscopy (*D*, *top panel*, *bright field image*; *bottom panel*, *fluorescence image*). *E* and *F*, glucose/ethylamine-grown HF290 cells (see *C* and *D*) were shifted to glycerol/methanol/ammonium sulfate medium and after 4 h of growth analyzed by immunocytochemistry for the location of Pex3p$_{1–50}$β−lactamase (α-β−lactamase and 5-nm GAR-gold) and Pex14p (α-Pex14p and 15-nm GAR-gold) (*E*) or BiP$_{1–30}$GFP (α-GFP and 5-nm GAR-gold) and Pex14p (α-Pex14p and 15-nm GAR-gold) (*F*). *M*, mitochondrion. *N*, nucleus. The *arrow* in *A* indicates the Pex3$_{1–50}$ vesicle cluster. The *arrows* in *F* indicate the 5-nm gold particles specific for BiP$_{1–30}$GFP. *Bar* = 0.5 μm (*A–C*), 5 μm (*D*), and 0.2 μm (*E* and *F*).

against *S. cerevisiae* BiP/Kar2p or Sec63p that cross-react with the *H. polymorpha* orthologues. However, these antisera showed insufficient specificity and/or labeling intensity in the immunocytochemical experiments and also on normal ER. Subsequently, we made use of an artificial marker for the *H. polymorpha* ER lumen. A hybrid protein, consisting of the

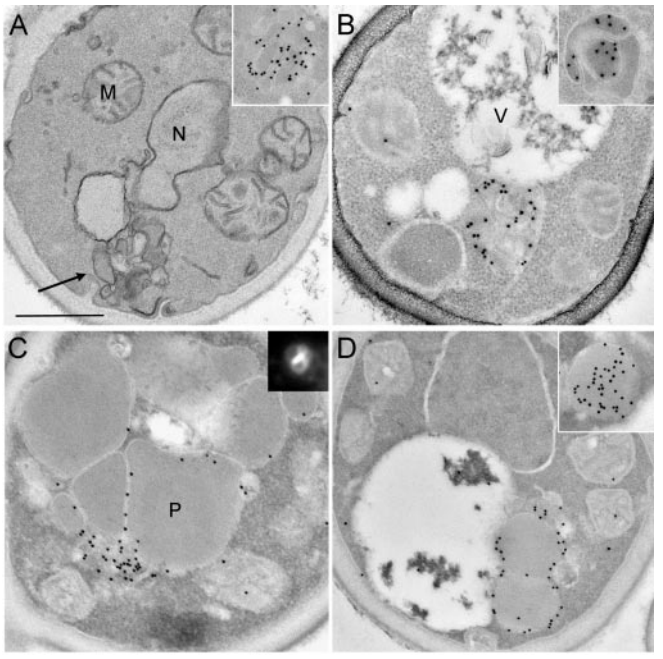

FIG. 7. **Pex3p$_{1–50}$ vesicles are the template for peroxisome biogenesis.** Electron microscopic analysis of HF245 (*pex3*::P$_{AOX}$-*PEX3*::P$_{AMO}$-*PEX3*$_{1–50}$*GFP*) cells shifted from glucose/ethylamine medium to glycerol/methanol/ammonium sulfate medium. *A* and *B*, 6 h after the shift; *C* and *D*, 16 h after the shift. *A*, morphology; *B–D* and *insets*, immunolocalization of Pex3p$_{1–50}$GFP (*A inset*, *C*); *B* and *D*, Pex3p; and *B inset* and *D inset*, AOX. Pex3p and AOX are sorted to the Pex3p$_{1–50}$GFP vesicle clusters (*B*). 16 h after the shift, significant amounts of Pex3p$_{1–50}$GFP is found on the peroxisomal membrane (*C*). The *inset* in *C* shows a fluorescent image of HF245 cells 14 h after the shift to methanol/ammonium sulfate medium. *M*, mitochondrion; *N*, nucleus; *P*, peroxisome; *V*, vacuole. The *arrow* in *A* and *E* indicates the Pex3p$_{1–50}$ vesicle cluster. *Bar* = 0.5 μm (similar magnifications were used for *A–D*).

N-terminal 30 amino acids of *H. polymorpha* BiP and containing its ER sorting signal, and GFP was synthesized in HF290 cells (*pex3*::P$_{AMO}$-*BiP*$_{1–30}$*GFP*::P$_{AOX}$-*PEX3*$_{1–50}$*β-lactamase*) under control of the amine oxidase promoter.[2] Fluorescence microscopic analysis of glucose/ethylamine-grown HF290 cells showed distinct staining of the nuclear envelope together with small patches at the cellular periphery (Fig. 6*D*). Immunocytochemical analysis showed that in these cells, α-GFP-specific labeling was confined to the nuclear membrane and the lateral ER (Fig. 6*C*). Next, these cells were shifted to glycerol/methanol/ammonium sulfate-medium, inducing the synthesis of Pex3p$_{1–50}$β-lactamase and fully repressing further synthesis of BiP$_{1–30}$GFP. Four hours after the shift, these cells were prepared for immunocytochemistry. As expected, synthesis of Pex3p$_{1–50}$β-lactamase caused the development of Pex3p$_{1–50}$ vesicles at the nuclear membrane. These vesicles contained both the Pex3p$_{1–50}$β-lactamase hybrid protein as well as endogenous Pex14p as shown by double-labeling experiments (Fig. 6*E*). The Pex3p$_{1–50}$ vesicles also contain significant α-GFP-specific labeling (Fig. 6*F*, 5-nm gold particles) suggesting that the artificial marker for the nuclear membrane/ER had incorporated in these vesicles under conditions that its synthesis was fully repressed. Taken together, these data suggest that the Pex3p$_{1–50}$ vesicles may be derived from the nuclear membrane/ER.

Pex3p$_{1–50}$ Vesicles Are the Target for Normal Peroxisome Development—Since the Pex3p$_{1–50}$ vesicles have peroxisomal characteristics, the next question we investigated is whether

[2] M. van der Heide and M. Veenhuis, unpublished data.

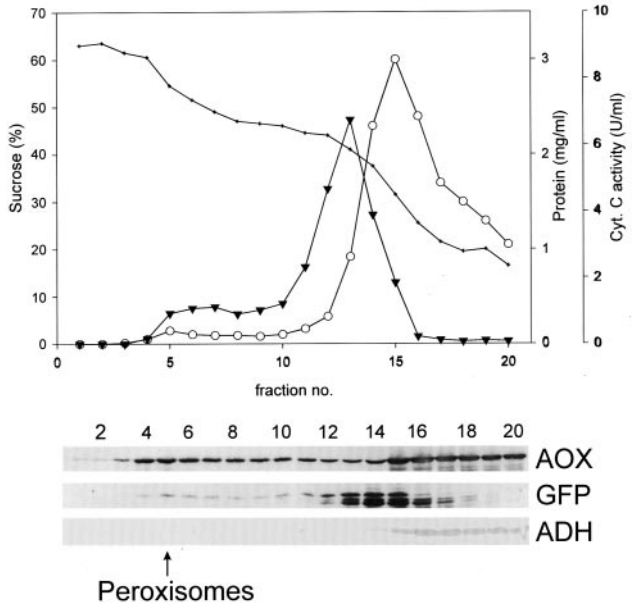

FIG. 8. **Peroxisomes of shifted HF245 cells contain Pex3p$_{1-50}$GFP.** The sucrose density gradient centrifugation of a PNS obtained from HF245 (*pex3*::P$_{AOX}$-*PEX3*::P$_{AMO}$-*PEX3*$_{1-50}$*GFP*) cells pregrown in glucose/ethylamine medium, shifted to methanol/ammonium sulfate medium and harvested at 22 h after the shift is shown. Individual fractions were analyzed for sucrose density (+), protein concentration (○), mitochondrial cytochrome *c* oxidase activity (▼), and cytosolic ADH protein (Western blot). Western blot analysis on individual fractions shows co-localization of AOX and Pex3p$_{1-50}$GFP at a sucrose density (54%) typical for WT peroxisomes. In addition, significant amounts of Pex3p$_{1-50}$GFP were found at sucrose concentrations of ~40%, indicating that Pex3$_{1-50}$ vesicles are still present in these cells. Also AOX was found at the top of the gradient due to leakage of matrix proteins from damaged peroxisomes during the isolation procedure.

they can act as precursors for peroxisome biogenesis after reintroduction of Pex3p in these cells. HF245 cells were precultivated in glucose/ethylamine-medium to induce Pex3p$_{1-50}$ vesicle formation. Subsequently, these cells were incubated for 30 min in glucose-ammonium sulfate medium to deplete the amine-induced mRNAs. After this incubation, the Pex3p$_{1-50}$ GFP mRNA level had dropped ~1,000-fold as determined by reverse transcription-PCR (data not shown). Next, the HF245 cells were transferred to methanol/ammonium sulfate medium, thus inducing Pex3p synthesis under conditions that fully repress Pex3p$_{1-50}$GFP synthesis. Samples were taken at regular time intervals from the HF245 culture and analyzed both biochemically and microscopically. Fig. 5*B* shows that after 1 h of incubation of these cells in fresh methanol/ammonium sulfate medium, Pex3p is readily detectable at levels that are slightly higher than those in WT cells grown on glucose/ammonium sulfate (comparison to WT not shown). The high initial levels of Pex3p$_{1-50}$GFP at $t = 0$ (glucose/ethylamine) only gradually decreased after the shift (Fig. 5*B*), suggesting that under these conditions no active degradation occurs of the Pex3p$_{1-50}$ vesicles. To analyze the mode and kinetics of peroxisome reappearance, samples taken at various time points after the shift of cells to methanol were prepared for electron microscopical analyses. As expected, the glucose/ethylamine-grown inoculum cells ($t = 0$) solely harbored GFP-containing vesicles and lacked peroxisomes (not shown, *cf*. Fig. 1). Four to six h after the shift, some vesicles within the Pex3p$_{1-50}$-membrane clusters had increased in size (Fig. 7, *A* and *B*). Immunocytochemical staining experiments revealed that AO protein was present in these enlarged compartments (Fig. 7*B*, *inset*). In contrast, Pex3p$_{1-50}$ GFP (Fig. 7*A*, *inset*) and Pex3p (Fig. 7*B*) were present throughout the whole population of vesicles, not restricted to the membranes of the enlarged vesicles. This suggests that all vesicles apparently initially accumulated Pex3p. However, not all vesicles developed into peroxisomes as indicated by the observation that after prolonged incubation of strain HF245 in methanol media, relatively few (3–6) peroxisomes had developed (Fig. 7, *C* and *D*) compared with the number of vesicles that were originally present. Anti-GFP- (Fig. 7*C*) and Pex3p- (Fig. 7*D*) dependent labeling was observed on the membranes of these organelles that were characterized by the presence of AO protein (Fig. 7*D*, *inset*). The presence of the GFP marker protein on peroxisomes could also be observed by fluorescence microscopy (Fig. 7*C*, *inset*). Since the expression of Pex3p$_{1-50}$ GFP was fully repressed under these conditions, these data suggest that the newly formed peroxisomes had developed from the Pex3p$_{1-50}$GFP-containing vesicles.

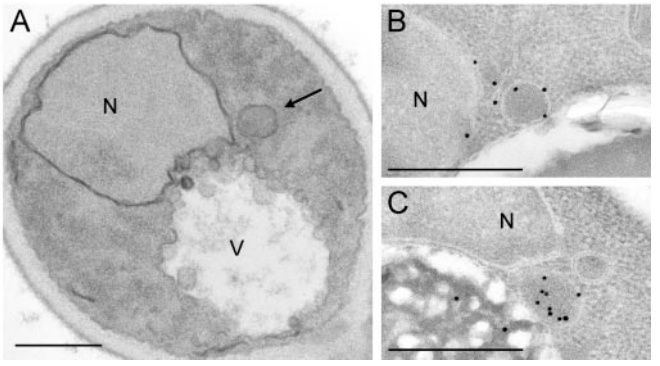

FIG. 9. **Peroxisomes arise at the nuclear membrane upon complementation of pex3 cells.** *A–C*, electron microscopical analysis of RBG17 (*pex3*::P$_{AOX}$-*PEX3*) cells 2 h after a shift from glucose/ethylamine medium to methanol/ammonium sulfate medium. *A*, morphology. *B* and *C*, immunolocalization of Pex3p (*B*) and AOX (*C*). *N*, nucleus. *V*, vacuole. The *arrow* in *A* indicates a newly formed peroxisome. *Bar* = 0.5 μm.

Subsequently, biochemical experiments were performed on HF245 cells, grown for 22 h after a shift from glucose/ethylamine medium to methanol/ammonium sulfate medium. Upon gradient centrifugation of cell homogenates minor, but significant, amounts of Pex3p$_{1-50}$GFP were detected in the peroxisomal peak fraction (at 54% sucrose), where also AO protein had accumulated (Fig. 8). Taken together, these data suggest that the Pex3p$_{1-50}$ vesicles can act as a template for peroxisome development after subsequent reintroduction of Pex3p.

Complementation of pex3 Cells by Full-length Pex3p Initiates with a Single Peroxisome—In control experiments, we analyzed peroxisome recovery in *pex3* cells upon complementation by the *PEX3* gene in the absence of Pex3p$_{1-50}$ vesicles. Electron microscopy showed that peroxisomes arose within 1 h after the shift of cells to inducing conditions. Invariably, only a single organelle was formed, located in the vicinity of the nuclear membrane (Fig. 9). The organelle was characterized by the presence of Pex3p (Fig. 9*B*) and AO (Fig. 9*C*). However, we never observed any proliferation of vesicles or additional membranes at the initial hours of peroxisome reintroduction comparable with Pex3p$_{1-50}$-producing cells. This indicates that the morphological events of peroxisome reintroduction in *pex3* cells significantly differ from those in similar cells that produce Pex3$_{1-50}$ protein.

DISCUSSION

Pex3p is a peroxisomal membrane protein essential for peroxisome biogenesis and maintenance of the organellar membrane (14, 16, 17, 21, 40). Previously, we reported that the first 50 amino acids of Pex3p are sufficient to target a reporter protein to the peroxisomal membrane (16, 27). Here we show that the same fragment of the protein is capable of inducing vesicle formation in *pex3* cells. These vesicles develop in the

vicinity of the nuclear membrane and preferentially served as templates for peroxisome development upon subsequent reintroduction of the full-length Pex3p. These data imply that the $Pex3p_{1–50}$ vesicles may be considered as an incomplete peroxisomal compartment that may be "trapped" in its maturation because of the absence of essential functions in the missing C-terminal part (amino acids 51–457) of Pex3p.

The current view of peroxisome proliferation predicts that new peroxisomes form from preexisting ones (9). However, this model can not explain some recent observations. Specifically, newly formed peroxisomes in peroxisome-deficient cells lacking any detectable peroxisomal (membrane) remnants (human and yeast *pex3* cells, human *pex16*, human and *S. cerevisiae pex19* cells) require an alternative membrane origin upon introduction of the complementing gene. Also, in *Y. lipolytica* and in plant cells, several peroxisomal membrane proteins have been proposed to travel via the ER or an ER-like compartment before reaching the peroxisome (10, 12). Whether this mechanism is generally valid, remains to be elucidated. In *H. polymorpha* an ER-to-peroxisome sorting pathway may exist, exemplified by the finding that a hybrid protein consisting of the 16 N-terminal amino acids of Pex3p fused to a reporter protein (PTS1-less catalase) is targeted to the nuclear membrane (16). The $Pex3p_{1–50}$-GFP-induced vesicles described in this study may concentrate at certain subdomains of the apparent donor membrane compartment, the nuclear membrane. Remarkably, upon induction solely the vesicles displayed fluorescence; invariably no nuclear or ER fluorescence was detected. The finding that only vesicles showed fluorescence lends support to the notion that they may not or hardly contain typical ER characteristics. Further evidence that the $Pex3p_{1–50}$ vesicles may indeed originate from the endomembrane system comes from the observation that they contained an overproduced ER-lumen protein, $BiP_{1–50}$GFP.

The $Pex3p_{1–50}$ vesicles contain at least one other peroxin, Pex14p, a protein that is missorted to mitochondria in *pex3* cells (21, 27). Because most peroxins in *H. polymorpha* are low abundant and therefore difficult to detect at endogenous levels, we have not been able to show conclusively that other peroxins are also present on these vesicles. The $Pex3p_{1–50}$ vesicles have, however, also acquired a typical property of WT *H. polymorpha* peroxisomes in that they are susceptible to selective degradation (38).

Interestingly, also in mammalian *pex3* cells a hybrid protein consisting of the N-terminal 40 amino acids of rat Pex3p and GFP is observed in vesicular structures (41). These vesicles were, however, not further characterized, thus it remains to be determined whether also these structures have peroxisomal features.

The key question to be answered was: are the $Pex3p_{1–50}$ vesicles a preferred target for peroxisome reintroduction upon synthesis of Pex3p? Using a *H. polymorpha* strain, in which vesicle formation and peroxisome biogenesis can be separately regulated, we were able to show that the vesicles population accumulated Pex3p, while only few of these incorporated the peroxisomal matrix protein AO. The possibility that the synthesis of Pex3p itself induces formation of new vesicle-clusters that mix with the preexisting $Pex3p_{1–50}$GFP vesicles is not very likely, because such vesicles were not observed when under identical conditions peroxisomes were reintroduced in *pex3* cells in the absence of $Pex3p_{1–50}$ vesicles (16) (see also Fig. 9).

Our data support the notion that 1) a Pex3p-receptor moiety is likely to exist on the endomembrane system of *pex3* cells and, subsequently, on the $Pex3p_{1–50}$-induced vesicles and 2) $Pex3p_{1–50}$ vesicles may act as a template for the assembly of peroxisomes. Most likely, incorporation of Pex3p solely does not restore the import of peroxisomal matrix proteins into these vesicles, and hence a further development of these vesicles (*e.g.* by the uptake of other essential proteins) is required for this. The details of this process, however, remain to be resolved. It can be envisaged that the endogenous levels of such proteins may be too low to complement all vesicles, and, in line with this, the transformation of some of the vesicles into peroxisomes may simply occur by chance.

In recent studies Titorenko and co-workers described the function of preperoxisomal vesicles in peroxisome biogenesis in WT *Y. lipolytica* cells (13, 42). Five subpopulations (P1–P5) with different biochemical characteristics were discriminated in a high-speed (200,000 × *g*) pellet fraction of a postnuclear supernatant after removing the mature peroxisomes during a low-speed (20,000 × *g*) centrifugation step. After a Pex1p- and Pex6p-dependent fusion of P1 and P2, they found that the resultant P3 was a precursor for P4, leading via P5 to mature peroxisomes, implying a prescribed maturation machinery for peroxisomes to become physiologically functional.

Other researchers have questioned the existence of vesicle-mediated, ER-to-peroxisome sorting pathways. Experiments on *S. cerevisiae* Pex15p, suggested that this protein was sorted via the ER, primarily because overproduction of the protein in WT cells caused massive overproliferation of ER membranes (karmellae; Ref. 43). In a recent study, however, it was shown that endogenous Pex15p remains cytosolic in *pex3* cells, whereas overproduced Pex15p again, gave rise to karmellea formation in these cells (40). This led the authors to conclude that the nuclear and ER localization of the protein, as well as the karmellae formation, may represent an artifact due to Pex15p overproduction.

In human cells, no evidence was obtained for routing of Pex16p via the ER. Like *pex3* cells, human cells lacking functional Pex16p, do not contain peroxisomal ghosts. Reappearance of peroxisomes in *pex16*-mutant cells upon reintroduction of the *PEX16* gene was not inhibited by brefeldin A and occurred normally at 15 °C, conditions that block COPII-mediated protein exit from the ER and COPI-mediated transport from the ER/Golgi intermediate compartment, respectively (20). Essentially similar results have recently been reported for peroxisome rescue in human *pex3* cells upon reintroduction of the complementing gene (21). These authors proposed a two-pathway model of peroxisome biogenesis. These include one pathway confirming the widely accepted view that peroxisomes arise by the growth and division of preexisting ones (9) and an alternative pathway by which peroxisomes form from a preperoxisomal vesicle. Their analyses, however, gave no clue as to whether such preperoxisomal structure exists or whether peroxisomes arise from the endomembrane system.

In WT *H. polymorpha* cells we have at present no direct evidence for a constitutive process invoking a role of ER vesicles in peroxisome biogenesis. However, our present observations suggest that specific vesicles derived from the endomembrane system or nuclear membrane may develop into normal peroxisomes. These data lend support to the view that in WT conditions sorting of Pex3p via the ER might be redundant and that, upon induction by growth compounds, peroxisomes normally develop by growth and fission. However, in cases where peroxisomes are lost, *e.g.* due to chemical-induced damage or failure in inheritance, formation of the organelles might be rescued and initiated at the endomembrane system.

Acknowledgments—We thank Dr. W.-H. Kunau (Ruhr University, Bochum, Germany) for the generous gift of antibodies against GFP and ADH and Dr. R. Schekman (University of California, Berkeley, CA) for the generous gift of antibodies against Sec63p.

REFERENCES

1. Veenhuis, M. (1992) *Cell Biochem. Funct.* **10,** 175–184
2. Kunau, W. H. (1998) *Curr. Opin. Microbiol.* **1,** 232–237
3. Erdmann, R., Veenhuis, M., and Kunau, W. H. (1997) *Trends Cell Biol.* **7,** 400–407
4. Subramani, S. (1998) *Physiol. Rev.* **78,** 171–188
5. Hettema, E. H., Distel, B., and Tabak, H. F. (1999) *Biochim. Biophys. Acta* **1451,** 17–34
6. Braverman, N., Dodt, G., Gould, S. J., and Valle, D. (1995) *Hum. Mol. Genet.* **4,** 1791–1798
7. Wanders, R. J. (1999) *Neurochem. Res.* **24,** 565–580
8. Fujiki, Y., Rachubinski, R. A., and Lazarow, P. B. (1984) *Proc. Natl. Acad. Sci. U. S. A.* **81,** 7127–7131
9. Lazarow, P. B., and Fujiki, Y. (1985) *Annu. Rev. Cell Biol.* **1,** 489–530
10. Titorenko, V. I., and Rachubinski, R. A. (1998) *Trends. Biochem. Sci.* **23,** 231–233
11. Faber, K. N., Heyman, J. A., and Subramani, S. (1998) *Mol. Cell. Biol.* **18,** 936–943
12. Mullen, R. T., Lisenbee, C. S., Miernyk, J. A., and Trelease, R. N. (1999) *Plant Cell* **11,** 2167–2185
13. Titorenko, V. I., Chan, H., and Rachubinski, R. A. (2000) *J. Cell Biol.* **148,** 29–44
14. Hohfeld, J., Veenhuis, M., and Kunau, W. H. (1991) *J. Cell Biol.* **114,** 1167–1178
15. Waterham, H. R., Titorenko, V. I., Swaving, G. J., Harder, W., and Veenhuis, M. (1993) *EMBO J.* **12,** 4785–4794
16. Baerends, R. J. S., Rasmussen, S. W., Hilbrands, R. E., van der Heide, M., Faber, K. N., Reuvekamp, P. T., Kiel, J. A. K. W., Cregg, J. M., van der Klei, I. J., and Veenhuis, M. (1996) *J. Biol. Chem.* **271,** 8887–8894
17. Wiemer, E. A. C., Luers, G. H., Faber, K. N., Wenzel, T. J., Veenhuis, M., and Subramani, S. (1996) *J. Biol. Chem.* **271,** 18973–18980
18. Götte, K., Girzalsky, W., Linkert, M., Baumgart, E., Kammerer, S., Kunau, W. H., and Erdmann, R. (1998) *Mol. Cell. Biol.* **18,** 616–628
19. Matsuzono, Y., Kinoshita, N., Tamura, S., Shimozawa, N., Hamasaki, M., Ghaedi, K., Wanders, R. J., Suzuki, Y., Kondo, N., and Fujiki, Y. (1999) *Proc. Natl. Acad. Sci. U. S. A.* **96,** 2116–2121
20. South, S. T., and Gould, S. J. (1999) *J. Cell Biol.* **144,** 255–266
21. South, S. T., Sacksteder, K. A., Li, X., Liu, Y., and Gould, S. J. (2000) *J. Cell Biol.* **149,** 1345–1360
22. van Dijken, J. P., Otto, R., and Harder, W. (1976) *Arch. Microbiol.* **111,** 137–144
23. Sambrook, J., Fritsch, E. F., and Maniatis, T. (1989) *Molecular Cloning: A Laboratory Manual*, Cold Spring Harbor Laboratory Press, Cold Spring Harbor, NY,
24. Faber, K. N., Haima, P., Gietl, C., Harder, W., AB, G., and Veenhuis, M. (1994) *Proc. Natl. Acad. Sci. U. S. A.* **91,** 12985–12989
25. Faber, K. N., Haima, P., Harder, W., Veenhuis, M., and AB, G. (1994) *Curr. Genet.* **25,** 305–310
26. Kiel, J. A. K. W., Keizer-Gunnink, I., Krause, T., Komori, M., and Veenhuis, M. (1995) *FEBS Lett.* **377,** 434–438
27. Baerends, R. J. S., Faber, K. N., Kram, A. M., Kiel, J. A. K. W., van der Klei, I. J., and Veenhuis, M. (2000) *J. Biol. Chem.* **275,** 9986–9995
28. Salomons, F. A., Kiel, J. A. K. W., Faber, K. N., Veenhuis, M., and van der Klei, I. J. (2000) *J. Biol. Chem.* **275,** 12603–12611
29. Faber, K. N., Keizer-Gunnink, I., Pluim, D., Harder, W., AB, G., and Veenhuis, M. (1995) *FEBS Lett.* **357,** 115–120
30. Laemmli, U. K. (1970) *Nature* **227,** 680–685
31. Kyhse-Andersen, J. (1984) *J. Biochem. Biophys. Methods* **10,** 203–209
32. Douma, A. C., Veenhuis, M., de Koning, W., Evers, M. E., and Harder, W. (1985) *Arch. Microbiol.* **143,** 237–243
33. van der Klei, I. J., Hilbrands, R. E., Kiel, J. A. K. W., Rasmussen, S. W., Cregg, J. M., and Veenhuis, M. (1998) *EMBO J.* **17,** 3608–3618
34. Douma, A. C., Veenhuis, M., Sulter, G. J., and Harder, W. (1987) *Arch. Microbiol.* **147,** 42–47
35. Waterham, H. R., Titorenko, V. I., Haima, P., Cregg, J. M., Harder, W., and Veenhuis, M. (1994) *J. Cell Biol.* **127,** 737–749
36. Bendayan, M. (1982) *J. Histochem. Cytochem.* **30,** 81–85
37. Veenhuis, M., Douma, A. C., Harder, W., and Osumi, M. (1983) *Arch. Microbiol.* **134,** 193–203
38. Veenhuis, M., Komori, M., Salomons, F. A., Hilbrands, R. E., Hut, H., Baerends, R. J. S., Kiel, J. A. K. W., and van der Klei, I. J. (1996) *FEBS Lett.* **383,** 114–118
39. van der Klei, I. J., Harder, W., and Veenhuis, M. (1991) *Yeast* **7,** 813–821
40. Hettema, E. H., Girzalsky, W., van den Berg, M., Erdmann, R., and Distel, B. (2000) *EMBO J.* **19,** 223–233
41. Ghaedi, K., Tamura, S., Okumoto, K., Matsuzono, Y., and Fujiki, Y. (2000) *Mol. Biol. Cell* **11,** 2085–2102
42. Titorenko, V. I., and Rachubinski, R. A. (2001) *Trends Cell Biol.* **11,** 22–29
43. Elgersma, Y., Elgersma-Hooisma, M., Wenzel, T. J., McCaffery, J. M., Farquhar, M. G., and Subramani, S. (1998) *J. Cell Biol.* **140,** 807–820
44. Gleeson, M. A. G., and Sudbery, P. E. (1988) *Yeast* **4,** 293–303